MicroRNA expression profile of gastrointestinal stromal tumors (GISTs)

Hee Jung Choi

Department of Medical Science

The Graduate School, Yonsei University

MicroRNA expression profile of gastrointestinal stromal tumors (GISTs)

Directed by Professor Hoguen Kim

The Master's Thesis
submitted to the Department of Medical Science,
the Graduate School of Yonsei University
in partial fulfillment of the requirements for the degree
of Master of Medical Science

Hee Jung Choi

December 2009

This certifies that the Master's Thesis
of Hee Jung Choi is approved.

Thesis Supervisor: Hoguen Kim

Thesis Committee Member: Jae Myun Lee

Thesis Committee Member: Won Sang Park

The Graduate School
Yonsei University

December 2009

ACKNOWLEDGEMENTS

다시 학문을 접했을 때 모든 것이 낯설고 신기했습니다. 처음부터 시작하는 저에게 지난 2년이라는 시간은 그 무엇과도 바꿀 수 없는 소중한 시간이었습니다.

저에게 많은 조언과 격려를 해주신 분들께 감사 인사 드립니다.

먼저 부족한 저에게 많은 용기와 배움을 주신 김호근 교수님. 정말 감사 드립니다. 또한 논문 심사에 큰 힘을 주신 이재면 교수님과 박원상 교수님께 진심 어린 감사를 드립니다.

아무것도 모르고 처음 실험실에 왔을 때 진지하게 가르쳐 준 권태, 그 누구보다 똘망똘망하게 자신이 해야 할 일을 잘 알고 열심히 하는 한나, 성실하게 실험실 살림까지 꼼꼼히 하는 나라, 먼 타국에서 오로지 연구를 위해 이곳에서 열심히 하는 모습 보여주는 미영, 이제 막 시작한 원규, 그 누구보다 착하고 귀여운 민지, 이번 논문을 쓰는데 많은 도움을 주신 권지은 선생님, 김현기 선생님, 그리고 이환석 선생님. 실험실 식구들 모두 너무 감사 드립니다.

대학시절부터 제 삶에 많은 조언을 해준 기청오빠, 다시 공부를 시작할 수 있도록 용기를 주고 바른 말로 큰 힘이 되어준 친구

효정이, 언제나 제게 즐거움을 가득 주는 유쾌한 친구 미선이, 내가 원하는 일을 할 수 있도록 충고와 격려를 아끼지 않은 혜정언니와 민숙언니에게도 감사 드립니다.

항상 딸을 믿어주시고 묵묵히 응원해주시는 사랑하는 아빠, 엄마. 힘들고 어려워도 두 분께서 옆에 계셔서 포기하지 않고 할 수 있었습니다. 진심으로 감사 드립니다. 그리고 사랑합니다. 때로는 친구처럼 때로는 오빠처럼 존재만으로도 든든한 하나뿐인 남동생 재석이에게 제 사랑과 감사를 드립니다.

이 모든 경험과 지식을 가슴속 깊이 간직하여 더 넓은 세상에서 당당하게 제가 맡은 일을 성실히 수행하는 연구자가 되겠습니다.

저자 씀

<TABLE OF CONTENTS>

LIST OF FIGURES

LIST OF TABLES

<ABSTRACT>

MicroRNA expression profile of gastrointestinal stromal tumors (GISTs)

Hee Jung Choi

Department of Medical Science
The Graduate School, Yonsei University

(Directed by Professor Hoguen Kim)

MicroRNAs are known to regulate gene expression. Although unique microRNA expression profiles have been reported in several tumors, little is known about microRNA expression profiles in GISTs. To evaluate the relationship between microRNA expression and clinicopathologic findings of GISTs, I analyzed the microRNA expression profiles of GISTs. I used fresh frozen tissues from 20 GISTs and analyzed *KIT* and *PDGFRA* mutations and chromosomal loss status. MicroRNA expression was analyzed using a microRNA chip containing 470 microRNAs. Using unsupervised hierarchical clustering analysis, I found four distinct microRNA expression patterns in our 20 GISTs. Six GISTs that did not have 14q loss formed a separate cluster. In

the 14 GISTs with 14q loss, 5 small bowel GISTs formed a separate cluster, and the remaining 9 GISTs could be divided into two groups according to frequent chromosomal losses and tumor risk. I found 73 microRNAs that were significantly down-regulated in the GISTs with 14q loss; 38 of these microRNAs are encoded on 14q. I also found many microRNAs that were down-regulated in small bowel and high-risk group GISTs. Most of the microRNAs down-regulated in the high-risk group and small bowel GISTs are known to be involved in tumor progression, specifically by stimulating mitogen-activated protein kinase (MAPK) and the cell cycle. The microRNA expression patterns of GISTs are closely related to the status of 14q loss, anatomic site, and tumor risk. These findings suggest that microRNA expression patterns can differentiate several subsets of GISTs.

Key words: microRNA, gastrointestinal stromal tumor, *KIT*, loss of 14q, expression profile

MicroRNA expression profile of gastrointestinal stromal tumors (GISTs)

Hee Jung Choi

Department of Medical Science
The Graduate School, Yonsei University

(Directed by Professor Hoguen Kim)

Ⅰ. INTRODUCTION

The molecular features of gastrointestinal stromal tumors (GISTs) are among the best characterized of all human tumors.[1-4] Activating mutations of the v-kit Hardy-Zuckerman 4 feline sarcoma viral oncogene homolog (*KIT*), a member of the receptor tyrosine kinase III family, are the most common genetic events in GISTs. *KIT* mutations are known to be present in approximately 80% of GISTs[5-7] and result in the autophosphorylation of KIT, resulting in activation of downstream signaling pathways.[8-10] Gain-of-function mutations of platelet-derived growth factor receptor α (*PDGFRA*), another member of the receptor tyrosine kinase III family, are present in approximately 35% of GISTs that lack *KIT* mutations.[11] Activating mutations of *KIT* and *PDGFRA* are mutually exclusive, and mutations in *PDGFRA* are

regarded as an alternative oncogenic mechanism in GISTs.[11, 12]

The characteristic fragile genomic sites of GISTs are well-known. The most common and characteristic genomic change is the loss of the long arm of chromosome 14 (14q).[13, 14] The other well-known chromosomal alterations are deletions of chromosome 1p and 22q.[15-19] Loss of 14q is known to be present in approximately 70% of GISTs, has no relationship to tumor risk, and can be found in any type of GIST.[16, 20] The other chromosomal changes are relatively infrequent, but occur more frequently in high-risk GISTs.[15, 16, 21]

Although certain molecular changes are characteristic of GISTs, few of these molecular characteristics explain the biologic behavior of the tumor or are useful for molecular classification. In previous studies, I demonstrated that the gene expression profiles of GISTs are relatively homogeneous, and have some relationship to the absence or presence of 14q and *KIT* mutations.[12, 22] I could not, however, find any other relationship between the gene expression profile and biological behavior of GISTs. The microRNA expression profiles of GISTs have been compared to other types of sarcomas.[23] However, the microRNA expression characteristics of subsets of GISTs and their relationship to genetic and clinicopathologic factors are unknown. It has been reported that microRNA expression is related to tumorigenesis and the phenotypic expression of many tumors.[24-26] Therefore, a microRNA expression study of GISTs might contribute to their accurate molecular characterization and classification. In this study, I evaluated the microRNA expression patterns of GISTs and analyzed the relationship between these patterns and the molecular and clinicopathologic characteristics of GISTs.

Ⅱ. MATERIALS AND METHODS

1. Patients and tissue samples

Twenty GISTs were included in this study. All cases were identified in the Department of Pathology at Yonsei University Medical Center between August 1997 and June 2006 for molecular marker studies. Authorization for the use of these tissues for research purposes was obtained from the Institutional Review Board of Yonsei Medical Center. Some of the fresh specimens were obtained from the Liver Cancer Specimen Bank of the National Research Resource Bank Program of the Korea Science and Engineering Foundation of the Ministry of Science and Technology.

Among 20 GISTs, 10 samples had previously been used for chromosomal and proteome analysis.[12, 22, 27] Information on clinical features and tumor sites were obtained from hospital charts and clinicians. The subjects included 11 females and 9 males ranging in age from 26 to 76 years (Table 1). All of the patients had been operated on directly without neoadjuvant therapy. Conventional pathologic parameters (anatomic site, risk, and tumor size) were examined prospectively without prior knowledge of the molecular data. GISTs were divided into four groups based on tumor risk according to the criteria of Fletcher and colleagues.[28]

Table 1. Clinicopathologic and Genetic status in 20 GISTs

Case No.	Age/ gender	Mutation status		Tumor					Cell type	Immunohistochemistry[1]		Chromosome 14q loss[2]
		KIT	*PDGFRA*	Size (cm)	Site	Mitotic count (/50HPF)	% of tumor cells	Grade		KIT	CD34	
1	64/M	wild	D842V	3	stomach	1	80	low	mixed	2(1)	2	Y
2	63/F	wild	D842V	11	stomach	6	80	high	mixed	1	0	Y
3	51/M	wild	wild	11	small bowel	2	80	high	spindle	3	2	Y
4	26/M	wild	wild	5.5	stomach	1	90	low	spindle	0	3	N
5	54/F	F506_F508 ins	wild	2.7	small bowel	14	80	high	mixed	3	0	Y
6	47/M	A504_Y505 ins	wild	6.5	small bowel	6	90	intermediate	spindle	2	2	Y
7	36/F	M552_Y553 del	wild	4	stomach	8	80	intermediate	spindle	3	3	N
8	74/F	D579 del	wild	4	stomach	4	95	low	spindle	3	3	Y
9	76/F	V560 del	wild	8	stomach	4	95	intermediate	spindle	3	3	Y
10	45/M	T574_R586 ins	wild	10	stomach	1	95	intermediate	spindle	3	3	N
11	68/F	V559D	wild	5.5	stomach	6	80	high	spindle	3	3	Y
12	67/F	K550_Q556 del	wild	8.5	stomach	9	80	high	spindle	3	3	Y
13	60/F	Q575_R589 ins	wild	4	stomach	8	95	intermediate	spindle	3	2	N
14	42/F	L556_D569 ins	wild	33	stomach	4	95	high	spindle	3	3	Y
15	52/F	wild	wild	7.5	stomach	4	90	intermediate	spindle	3	3	N
16	65/M	A504_Y505 ins	wild	6.6	small bowel	23	95	high	spindle	3	0	Y
17	61/M	wild	D842V	20	stomach	6	80	high	mixed	1	1	Y
18	50/M	W557_K558 del	wild	8	stomach	23	95	high	mixed	3	3	Y
19	70/M	wild	D842V	2.5	stomach	0	80	low	mixed	1	3	N
20	68/F	A504_Y505 ins	wild	9	small bowel	20	95	high	mixed	3	0	Y

[1]Immunoscore; 0, no positive tumor cells; 1, under 10% tumor cells are positive. 2, between 10% and 50% tumor cells are positive. 3, more than 50% tumor cells are positive. - [2]N; no loss, Y; loss

2. Analysis of mutations in *KIT* and *PDGFRA*

I selected tumor tissues comprising more than 80% tumor cells by evaluating a validation block or frozen tissues. Somatic mutations in exons 9, 11, 13, and 17 of *KIT*, and mutations in exons 12 and 18 of *PDGFRA* were analyzed in my 20 GISTs using PCR-based assays as described previously.[5, 6, 8, 11, 29] The PCR products were sequenced using an ABI Prism 310 Genetic Analyzer (Applied Biosystems, Foster City, CA).

3. Loss of heterozygosity analysis

Loci of 1p, 14q, and 22q were PCR-amplified from DNA extracted from GISTs and matched normal tissues to evaluate the frequency and extent of deletions. PCR reactions were carried out in a volume of 20 μl containing 1.5 mmol/L $MgCl_2$, 20 pmol primer, 0.2 mmol/L of dATP, dGTP, and dTTP, 5 μmol/L dCTP, 1 μCi of [α-^{32}P] dCTP (3000 Ci/mmol; NEN DuPont, Boston, MA), 50 ng of sample DNA, 1x PCR buffer, and 1.25 U Taq polymerase (Gibco-BRL, Grand Island, NY). After denaturation at 95 °C for 5 minutes, DNA amplification was performed for 30 cycles of denaturation at 95 °C for 30 seconds, primer annealing at 55–60 °C for 30 seconds, and elongation at 72 °C for 15 seconds. The primer sequences for LOH analysis are listed in Table 2. PCR products were separated on 6% polyacrylamide gels containing 5.6 mol/L urea, followed by autoradiography. Allelic deletion was scored when the band intensity of one marker was significantly decreased (> 70% reduction) in the tumor DNA compared to the DNA from non-tumor tissue. To examine in detail the deletion status of chromosomes 1p, 14q, and 22q, we used 5, 14, and 7 microsatellite markers, respectively. I used DNA extracted

from matched normal tissues, namely grossly normal-looking mucosa or smooth muscle. The matched normal tissue was not available in one case (case 16), and an array CGH was used in two cases (cases 6 and 16). CGH was performed at LNC Bio Inc. (Seoul, Korea) using an Agilent Oligonucleotide Array-Based CGH for genomic DNA analysis (Version 2.0) (Agilent Technologies, Santa Clara, CA).

Table 2. Primer sequences for loss of heterozygosity analysis

Primer	Sequence
D14S582 F	5'-GGTTCTCCAGAGAAGCAGAA-3'
D14S582 R	5'-CAGGGCTTCTGATTCTTGAG-3'
D14S70 F	5'-ATCAATTTGCTAGTTTGGCA-3'
D14S70 R	5'-AGCTAATGACTTAGACACGTTGTAG-3'
D14S288 F	5'-AGCTAGACTCTGCCATAAACA-3'
D14S288 R	5'-TGGAGACAGGAACAACACAC-3'
D14S281 F	5'-GATGCTAGGGATGCCTGCTACT-3'
D14S281 R	5'-TGGCAGAATGTTAGACTGCTTCTT-3'
D14S283 F	5'-GGGACTATATCTCCCAGGC-3'
D14S283 R	5'-TGTTTTCCTAGTAACCGCA-3'
D14S285 F	5'-ACATGGCCCCCAAGTTT-3'
D14S285 R	5'-TGTTTTCCTAGTAACCGCA-3'
D14S980 F	5'-CTGGGCAACAAGAGTGG-3'
D14S980 R	5'-GAAGCGGGACAATTCTCTAAG-3'
D14S268 F	5'-AGCTTCCTACTGTGTAAAACGA-3'
D14S268 R	5'-GGGGCTGCACCTTGTA-3'
D14S67 F	5'-TCACTACGCCTCTACAATTCTATG -3'
D14S67 R	5'-TAGTCAGGGTTTGCCAGAGA-3'
D14S51 F	5'-ATGCTCAATGAACAGCCTGA-3'
D14S51 R	5'-GATTCTGCACCCCTAAATCC-3'
D14S267 F	5'-TTAATGCCCACTGAATGCT-3'
D14S267 R	5'-AAGGCAGCCCTGGTTT-3'
D14S1426 F	5'-CCTGGGCGACAGTAATGG-3'
D14S1426 R	5'-GGGAGAGGCCCTGTATTAGT-3'
D14S1203 F	5'-GCTACACAGCTGTCCTCTTGG-3'
D14S1203 R	5'-CCAAGGATTCATGTTGCATG-3'
D14S1006 F	5'-TTCCACAGGGCAAGCAGTA-3'
D14S1006 R	5'-TTCTGGCAAAACCCAACC-3'

4. RNA preparation and microarray analysis

Total RNA was extracted from frozen tissues using TRIZOL as per the manufacturer's instructions (Life Technology, Rockville, MD). One hundred micrograms of total RNA was used as input for small RNA isolation. To collect pure microRNA, I extracted the microRNA from total RNA using Microcon YM-3 and YM-100 columns (Millipore. Billerica, MA). The collected microRNA was labeled using a MessageAmp™Ⅱ-biotin Enhanced Kit (Ambion, Austin, USA) according to the manufacturer's instructions. After microRNA labeling, the RNAs were hybridized to the Homo Sapiens CombiMatrix chip (4 x 2K) (CombiMatrix Corp. Mukilteo, WA), which contains probe designs based on unique microRNA species from the current release of the Sanger database (Version 9.0 is at http://microrna.sanger.ac.uk/sequences). Hybridized microarrays were scanned using a pixel size of 5 and a focus position of 130 using a GenePix 4000B microarray scanner (Axon Instruments, Union City).

Data normalization was performed for all filtered microRNA probes with the exception of non-microRNA controls (such as the positive, negative, and degradation controls). This was followed by within-global scale factor normalization to ensure that all sample backgrounds had the same value. Average $\log_2$ ratios were calculated from the normalized data based on two measurements of each microRNA. RNA hybridization and scanning were performed by Macrogen Inc. (Seoul, Korea).

5. MicroRNA RT-PCR

Total RNA from eight cases was extracted from fresh frozen tissues using TRIZOL (Life Technology, Rockville, MD). One hundred micrograms of total RNA was used as input for small RNA isolation. cDNAs were generated using M-MLV Reverse Transcriptase (Invitrogen, California, USA) according to the manufacturer's instructions. PCR reactions were carried out in a 20 μl mixture containing 1.5 mmol/L $MgCl_2$, 20 pmol primer, 2.5 mmol/L each dATP, dGTP, dTTP, and dCTP, 4 μg of cDNA, 10x PCR gold buffer, and AmpliTaq Gold® (Applied Biosystems). After denaturation at 95 °C for 10 minutes, DNA amplification was performed for 30 cycles of denaturation at 95 °C for 30 seconds, primer annealing at 55-60 °C for 30 seconds, and elongation at 72 °C for 30 seconds. The relative intensity of mRNA expression of each sample was then normalized against 5S RNA as a surrogate for total mRNA. miRNA primer sequences are listed in Table 3. Each of the PCR products (20 μl volume) was directly loaded onto a 3.5% agarose gel stained with ethidium bromide, and visualized directly under ultraviolet illumination.

Table 3. Primer sequences of microRNA RT-PCR analysis

MicroRNA	Sequence
miR-495 F	5'-GCCCATGTTATTTTCGCTTT -3'
miR-495 R	5'-TACCGAAAAAGAAGTGCACCA -3'
miR-376 F	5'-TTCTTTGGTATTTAAAACGTGGA-3'
miR-376 R	5'-GGAGAATCTACCTTTTACAGCATT -3'
miR-134 F	5'-TGTGACTGGTTGACCAGAGG -3'
miR-134 R	5'-GTGACTAGGTGGCCCACAG -3'
miR-377 F	5'-AGAGGGTGCCCTTGGTGAAT -3'
miR-377 R	5'-AACAAAAGTTGCCTTTGTGTGA -3'
miR-539 F	5'-ATCCTTGGTGTGTTCGCTTT -3'
miR-539 R	5'-CAAAAAGAAATTGTCCTTGTATGA -3'
5S RNA F	5'-TCTCGTCTGATCTCGGAAGC -3'
5S RNA R	5'-AGCCTACAGCACCCGGTATT -3'

6. Northern blot analysis of mRNA

Total RNAs (30 μg) from snap-frozen tissues were fractionated on a denaturing 15% TBE-UREA gel. The gel was then transferred to Hybond-N+ membranes (Amersham Biosciences, NY, USA) and fixed by ultraviolet cross-linking at 1200 μJ. Membranes were then hybridized overnight at 37 °C in ULTRAhyb-oligo (Ambion, TX, USA), together with a locked nucleic acid modified oligonucleotide probe complementary to the mature microRNAs that was labeled with T4 polynucleotide kinase (NEB) and γ-P^{32} ATP (Bio-Medical Science, Seoul, Korea). The sequences of probes are as follows: miR-377: 5'-ACAAAAGTTGCCTTTGTGTGAT-3', miR-154: 5'-AATAGGTCAACCGTGTATGATT -3'. The relative intensity of RNA expression of each sample was then normalized against 5S RNA. Subsequently, the blots were washed three times at 37 °C for 5 min each in 2x SSC/0.1% SDS. The blots were then incubated with the BAS cassette 2040 (Fuji photo film, Tokyo, Japan) and exposed to Fuji Medical X-ray film (Fuji photo film).

7. Western blot analysis of KIT

Whole lysates from tumor specimens were prepared using lysis buffer (50 mM Tris (pH 7.4), 1% Triton X-100, 5 mM EDTA, 1 mM KCl, 140 mM NaCl, 2 mM $MgCl_2$, 1 mM phenylmethylsulfonyl fluoride, 1 mM sodium fluoride, 1% aprotinin, 1 M leupeptin, and 1 mM sodium ortho-vanadate). Total protein lysates (20 μg) were loaded into each lane, size-fractionated by SDS–PAGE, and transferred to a polyvinylidene difluoride membrane that was blocked with Tris-buffered saline–Tween 20 containing 5% skim milk. Primary

antibody against KIT (1: 4000. Santa Cruz Biotech, Santa Cruz, CA, USA) and glyceraldehyde-3-phosphate dehydrogenase (GAPDH; 1:200,000. Trevigen, Gaitherburg, MD, USA) were incubated with the membranes for 1 h at room temperature. After washing, membranes were incubated with a secondary goat anti-rabbit IgG-HRP conjugated antibody (Santa Cruz Biotech) for anti-KIT and with a secondary rabbit anti-mouse IgG-HRP conjugated antibody (Santa Cruz Biotech) for anti-GAPDH, washed, and then developed using ECL-Plus reagents (Amersham Pharmacia Biotech, Uppsala, Sweden).

8. Immunohistochemical staining

Immunohistochemistry was performed using an avidin-biotin peroxidase complex system with diaminobenizidine (DAB) as the chromogen. Primary antibodies included c-kit (1:50, DAKO, Copenhagen, Denmark) and CD34 (1:50, DAKO, Copenhagen, Denmark).

Immunohistochemical results were evaluated semi-quantitatively as follows. Strong positivity: more than 10% of tumor cells moderately or strongly positive; weak positivity: less than 10% of tumor cells moderately or strongly positive, or more than 10% of the tumor cells, weakly positive; negative: less than 10% of tumor cells weakly positive for the stain or no positive cells.

9. Agglomerative hierarchical clustering

Unsupervised hierarchical clustering analysis was used to classify the 20 GISTs according to their gene expression patterns. I used a data set of genes that satisfied the following filtering criteria: genes with log-transformed ratio

values of more than 80% (across all arrays) were taken and genes with log-transformed ratio of less than 0.2 standard deviations were discarded. The selected gene data set was then analyzed using complete-linkage hierarchical clustering using the uncentered correlation similarity metric method in Cluster version 2.11. The expression map results were visualized with Treeview version 1.60 software (http://rana.lbl.gov/EisenSoftware.htm).

10. Identification of differentially expressed genes according to anatomic site, tumor risk, and loss of 14q

To detect differentially expressed microRNAs according to the anatomic site of the tumor, tumor risk, and loss of 14q status, 20 GISTs were classified and analyzed. I ranked the microRNAs using the Mann-Whitney rank sum test. Outlier genes responsible for anatomic site or chromosomal alteration status were selected by $p < 0.05$. In addition, significant outlier subset genes were further narrowed-down by filtering genes showing greater than ± 2-fold expression changes.

Ⅲ. RESULT

1. Clinicopathologic characteristics and mutation status of *KIT* and *PDGFRA* in GISTs

Among the 20 GISTs, 4 cases were categorized as low-risk, 6 cases as intermediate-risk, and 10 cases as high-risk according to NCI consensus criteria.[28] Fifteen cases were stomach GISTs and the remaining five cases were small bowel GISTs. Immunoreactivity for KIT and CD34 were present in 19 and 16 cases, respectively. Deletion of 14q was detected in 14 cases. *KIT* mutations were detected in 13 of 20 cases. In the 13 GISTs with *KIT* mutations, 9 mutations were present in exon 11, and 4 mutations were present in exon 9. Insertion mutations were most common, and were found in seven cases, while point mutations were found in one case and deletions were found in five cases. Among the remaining seven cases lacking *KIT* mutations, four cases had a *PDGFRA* mutation, and all mutations were point mutations in exon 18 (Table 1). Among 13 *KIT*-mutated GISTs, 10 had a spindle cell type and 3 had a mixed cell type; all 4 *PDGFRA*-mutated GISTs had a mixed cell type.

2. Unsupervised hierarchical clustering analysis distinguishes four subtypes of GISTs

I initially performed a molecular pattern analysis to identify different subsets of GISTs according to microRNA expression profiles. All array data for the samples described in this study can be accessed on our web page (http://www.molpathol.org). Using a relevant set of 363 pre-filtered genes (see

"Materials and Methods"), I conducted a complete-linkage hierarchical clustering analysis of 20 arrays. My microRNA expression study classified GISTs into four subgroups; a two-way hierarchical clustering analysis completely distinguished GISTs into two clusters and these two clusters were further divided into two additional clusters each (branches A, B, C, and D; Fig. 1). Cases in branch A and B were high-risk GISTs and had more frequent chromosomal losses than the cases in branches C and D. GISTs in branches A and B were separated by anatomic site (small bowel versus stomach). All five GISTs in branch A developed in the small bowel, while four GISTs in branch B were stomach GISTs. Furthermore, all the GISTs in branches C and D were stomach GISTs and were separated according to 14q loss. All six stomach GISTs without 14q loss formed a separate cluster in branch D. The mutation status of *KIT* or *PDGFRA*, clinicopathologic factors such as histological type, age, sex, and the immunohistochemical expression status of KIT or CD34 were not related to the microRNA expression pattern.

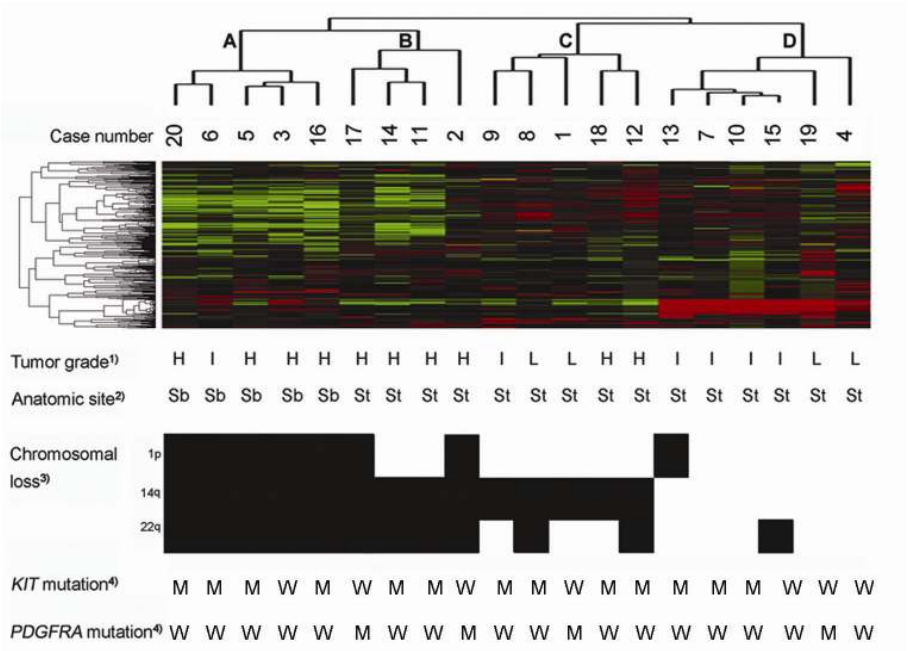

Fig 1. Unsupervised hierarchical clustering analysis of microRNA expression in 20 GISTs. A two-way hierarchical clustering analysis revealed two GIST clusters that were each divided into another two clusters. Branch A is composed of high-risk GISTs in the small bowel, while branch B contains high-risk stomach GISTs with frequent chromosomal changes. Branch C is composed of intermediate-risk stomach GISTs with 14q loss. All six stomach GISTs lacking 14q loss formed a separate cluster in branch D. The mutation status of *KIT* and *PDGFRA* was not related to the microRNA expression pattern. 1) H; high-risk group, I; intermediate-risk group, L; low-risk group. 2) Sb; small bowel, St; stomach. 3) Black box; chromosomal loss, White box; no chromosomal loss. 4) M; mutation positive, W; wild-type.

3. Differentially expressed microRNAs according to anatomic site and tumor risk

Because all five small bowel GISTs formed a separate cluster, I attempted to identify a robust set of anatomic site-related genes by a supervised rank-sum analysis using the Mann-Whitney rank sum test. To minimize the microRNA expression differences due to different clinical features and chromosomal changes, I selected nine GISTs in branches A and B (five small bowel GISTs and four stomach GISTs), and used a stringent selection criterion (See "Materials and methods"). Twenty-four microRNAs were found to be either up-regulated (4 genes) or down-regulated (20 genes) in the five small bowel GISTs compared to the four stomach GISTs. Examples of genes differentially expressed ($p < 0.05$, fold change > 2.5) in the small bowel and stomach GISTs are listed in Table 4.

Table 4. Differentially expressed microRNAs between 5 high-risk small bowel and 4 high-risk gastric GISTs

MicroRNA	Fold change[1]	Chromosome location	Predicted target genes[2]	Related pathway[3]
Up-regulated in small bowel GISTs				
miR-383	13.78	8	*EGF, PAK1*	MAPK ↓
miR-136	4.79	14	*ELK1, MOS*	MAPK ↓
miR-146a	4.22	5	*EGFR, TRAF2, TRAF6*	MAPK ↓
miR-409-3p	3.49	14	*CDK7*	Cell cycle ↓
Down-regulated in small bowel GISTs				
miR-124a	10.77	20	*RAF1*	MAPK ↑
miR-199b	10.33	9	*PAK1, TRAF2, NLK*	MAPK ↑
miR-451	8.25	17	*ELK1, RAF1*	MAPK ↑
miR-663	6.85	20	*PLK1*	Cell cycle ↑
miR-10a	6.28	17	*BDNF, SRF*	MAPK ↑
miR-218	5.67	5	*ATR*	Cell cycle ↓
miR-638	4.02	14	*BAX*	Apoptosis ↑
miR-24	3.51	19	*SRF, NLK*	MAPK ↑
miR-27b	3.24	9	*EGFR, GRB2, MEF2C*	MAPK ↑
miR-128b	3.24	3	*EGFR, GRB2*	MAPK ↑
miR-588	2.95	6	*IL10*	JAK-STAT ↑
miR-518c	2.88	19	*EGF, JUND*	MAPK ↑
miR-199a*	2.74	1	*SRF, NLK*	MAPK ↑
miR-346	2.68	10	*SMAD3, SMAD4*	Cell cycle ↓
miR-200a	2.60	1	*EGF, GRB2 / CDK6*	MAPK↑ / Cell cycle ↑
miR-526a	2.59	19	*BAD, BID*	Apoptosis ↑
miR-625	2.59	14	*BAD, BAX*	Apoptosis ↑
miR-489	2.57	7	*RAF1*	MAPK ↑
miR-140	2.53	16	*EGFR, NLK*	MAPK ↑
miR-23b	2.51	9	*MEF2C*	MAPK ↑

NOTE. [1]Average ratio of intensity of 5 high-risk small bowel GISTs / average ratio of intensity of 4 high-risk gastric GISTs (by using functional POWER (number is 2). $p < 0.05$, Fold change > 2.5). -[2]Predicted target genes in this table are represented in NCBI gene symbol. -[3]↑:up-regulated, ↓:down-regulated

I then analyzed which specific microRNAs were differentially expressed according to tumor risk. I compared 10 high-risk GISTs (6 gastric and 4 small bowel GISTs) to 4 low-risk GISTs (4 gastric GISTs), and found that 28 microRNAs ($p < 0.05$, fold change > 2.0; Table 5) were down-regulated in the high-risk GISTs. When I compared six high-risk gastric GISTs and four low-risk gastric GISTs, I found 32 microRNAs that were down-regulated in high-risk gastric GISTs ($p < 0.1$, fold change > 2.0). Among the 28 microRNAs that were down-regulated in high-risk GISTs, I found that 16 (16/28, 57.1%) microRNAs were also down-regulated in high-risk gastric GISTs. The remaining 12 microRNA were also down-regulated in high-risk gastric GISTs, although the values did not fulfill the statistical significance (Table 6).

Table 5. Differentially expressed microRNAs between 10 high-risk and 4 low-risk GISTs

MicroRNA	Fold change[1]	Chromosome location	Predicted target genes[2]	Related pathway[3]	Expected effect
Down-regulated in high risk GISTs					
miR-146b	7.75	5	*DAXX, EGFR, TRAF6*	MAPK ↑	apoptosis, proliferation
miR-150	5.52	19	*ELK1, PAK1*	MAPK ↑	proliferation, signal transduction
miR-132	4.46	17	*DAXX, GRB2, NLK*	MAPK ↑	apoptosis, proliferation, Wnt signaling
miR-342	4.20	14	*ELK1, TRAF2, CDC42*	MAPK ↑	proliferation,degradation, signal transduction
miR-16	4.13	3	*BCL2*	Apoptosis↓	anti-apoptotic
miR-500	3.84	X	*ELK1, NLK*	MAPK ↑	proliferation, Wnt signaling
miR-212	3.60	17	*DAXX, NLK*	MAPK ↑	apoptosis, Wnt signaling
miR-335	3.46	7	*SKP2, CDC7*	Cell cycle ↑	cell growth and death, DNA biosynthesis
miR-21	3.45	17	*DAXX*	MAPK ↑	apoptosis
miR-199a	3.35	1	*EGF, SRF, NLK*	MAPK ↑	proliferation, Wnt signaling
miR-424	3.33	X	*BDNF, CDC42, RAF1*	MAPK ↑	proliferation, signal transduction
miR-23b	3.26	9	*FAS, CASP3, CASP7*	Apoptosis ↑	Degradation
miR-487a	3.02	14	*RHOA, NLK*	Wnt ↑	cytoskeltal change, signal transduction
miR-107	3.02	10	*BDNF, CDC42, RAF1*	MAPK ↑	proliferation, signal transduction
miR-26b	2.94	9	*EGF, NLK, PAK1,2*	MAPK ↑	proliferation,Wnt sinaling signal transduction
miR-214	2.90	1	*CDC25B, PAK2*	MAPK ↑	signal transduction
miR-100	2.86	11	*CDK7, PLK1*	Cell cycle ↑	cell growth and death
miR-148b	2.84	12	*MAX, NLK*	MAPK ↑	apoptosis, Wnt signaling
miR-152	2.68	17	*MAX, NLK*	MAPK ↑	apoptosis, Wnt signaling
miR-125b	2.63	21	*EGF, SRF*	MAPK ↑	Proliferation
miR-30e-5p	2.63	1	*BDNF, PAK1*	MAPK ↑	proliferation, signal transduction
miR-485-3p	2.47	14	*RHOA, CUL1*	Wnt ↑	cytoskeltal change, signal transduction
miR-28	2.46	3	*MAX, SRF*	MAPK ↑	apoptosis, proliferation
miR-19a	2.30	13	*MEF2C, RAF1, SRF*	MAPK ↑	Apoptosis, proliferation
miR-15a	2.15	13	*BCL2*	Apoptosis↓	anti-apoptotic
miR-34b	2.13	11	*BCL2*	Apoptosis↓	anti-apoptotic
miR-362	2.11	X	*FAS, MEF2C*	MAPK ↑	Apoptosis, apoptosis
miR-126	2.01	9	*ATR, PLK1*	Cell cycle ↑	cell cycle arrest, cell growth and death

NOTE. [1]Average ratio of intensity of 10 high-risk GISTs / average ratio of intensity of 4 low-risk GISTs (by using functional POWER (number is 2). $p < 0.05$, Fold change > 2.0). -[2]Predicted target genes in this table are represented in NCBI gene symbol. - [3]↑: up-regulated, ↓: down-regulated

Table 6. Differentially expressed microRNAs between 6 high-risk and 4 low-risk gastric GISTs

MicroRNA	Fold change[1]	Chromosome location	Predicted target genes[2]	Related pathway[‡]
Down-regulated in high-risk gastric GISTs				
miR-377	12.32	14	*CD14, SRF*	MAPK↑
miR-409-3p	8.00	14	*CDK7*	cell cycle↓
miR-376a*	7.62	14	*BUB1, BUB3*	cell cycle↑
miR-376b	6.45	14	*FGFR1, RASA1*	MAPK↑
miR-127	6.43	14	*MAX, FGF3*	MAPK↑
miR-136	5.93	14	*ELK1, MOS*	MAPK↑
miR-150	5.66	19	*ELK1, PAK1*	MAPK↑
miR-495	5.23	14	*FGF14, IL1B, TGFB2*	MAPK↑
miR-154*	4.94	14	*RHOA*	Cell-matrix adhesion ↑
miR-497	4.94	17	*BDNF, FGFR4, RAF1*	MAPK↑
miR-381	4.19	14	*BDNF, SRF, NLK*	MAPK↑
miR-132	4.16	17	*DAXX, GBR2, NLK*	MAPK↑
miR-195	4.01	17	*BDNF, CDC42*	MAPK↑
miR-487b	3.98	14	*PAK7*	Cell-matrix adhesion ↑
miR-335	3.82	7	*SKP2, CDC7*	cell cycle↑
miR-146b	3.78	10	*DAXX, EGFR, TRAF6*	MAPK↑
miR-342	3.25	14	*ELK1, TRAF2, CDC42*	MAPK↑
miR-363*	2.98	X	*ILK*	Cell-matrix adhesion ↑
miR-100	2.98	11	*CDK7, PLK1*	cell cycle↑
miR-21	2.95	17	*DAXX*	cell cycle↑
miR-424	2.74	X	*BDNF, CDC42, RAF1*	MAPK↑
miR-214	2.62	1	*CDC25B, PAK2*	MAPK↑
miR-487a	2.56	14	*RHOA, NLK*	Wnt↑
miR-16	2.48	3	*BCL2*	Apoptosis↓
miR-133b	2.33	6	*CDC42, MOS*	MAPK↑
miR-140	2.28	16	*CDC42, EGFR*	MAPK↑
miR-125b	2.18	21	*EGF, SRF*	MAPK↑
miR-23b	2.16	9	*FAS, CASP3, CASP7*	Apoptosis↑
miR-365	2.13	17	*BDNF, ATF2*	MAPK↑
miR-30e-5p	2.10	1	*BDNF, PAK1*	MAPK↑
miR-152	2.04	17	*MAX, NLK*	MAPK↑
miR-26b	2.01	2	*EGF, NLK, PAK1,2*	MAPK↑

NOTE. [1]Average ratio of intensity of 6 high-risk / average ratio of intensity of 4 low-risk gastric GISTs (by using functional POWER (number is 2). $p < 0.1$, Fold change > 2.0). -[2] Predicted target genes in this table are represented in NCBI gene symbol. - [3]↑: up-regulated, ↓: down-regulated

4. Differentially expressed microRNAs according to 14q loss

My study found that six GISTs without 14q loss formed a separate cluster (Fig. 1, branch D). When I analyzed the chromosomal loss status of 14q by deletion mapping, 13 GISTs showed total loss while 1 GIST showed partial loss (Fig 2).

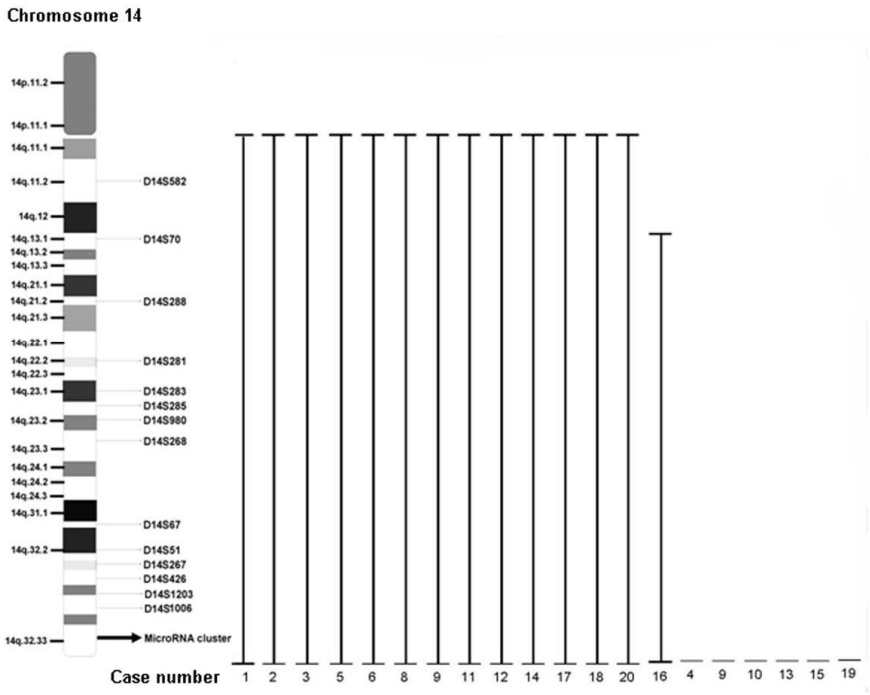

Fig 2. Loss of heterozygosity (LOH) mapping of chromosome 14q. Chromosomal loss is indicated as black line. Thirteen out of 14 cases showed total loss of 14q and one case (case 16) showed partial loss.

The GIST with the partial 14q loss (case 16) was a small bowel GIST with an intact proximal chromosome fragment of 14q (Fig 3).

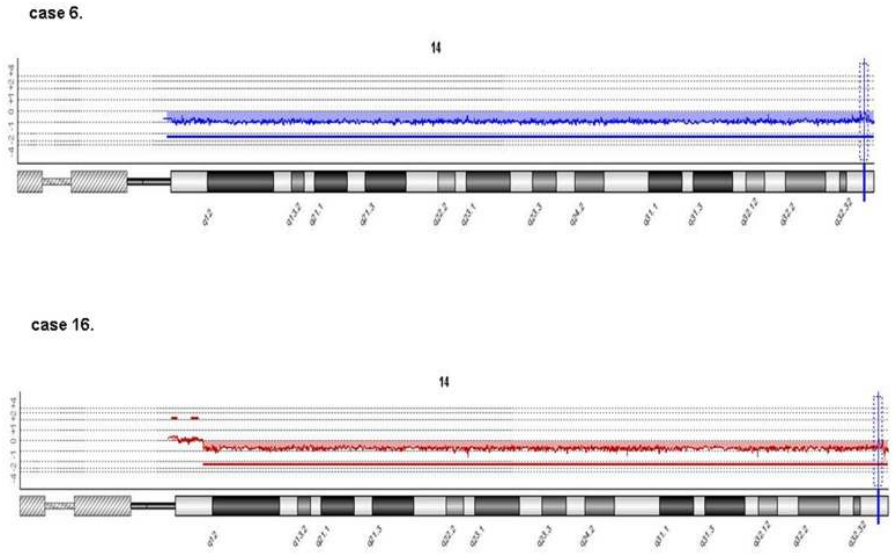

Fig 3. Array CGH analysis of chromosome 14q of case 6 and case 16. Array CGH demonstrated total loss of 14q in case 6, and partial loss in case 16.

I then analyzed the differently expressed microRNAs according to 14q loss status. In total, a subset of 73 microRNAs was at a significant level differentially expressed between GISTs with 14q loss and GISTs without 14q loss. Among the 73 microRNAs, 38 microRNAs were encoded by 14q. When I analyzed the expression profiles of the 73 microRNAs using supervised hierarchical clusters analysis, I found that there was a trend of GISTs grouping according to anatomic site (Fig. 4*a*).

I further analyzed the 38 down-regulated microRNAs located at

chromosome 14q. In chromosome 14q, two loci of microRNA clusters are present near the distal end, 14q 32.33. Among these two clusters, the proximal locus has 10 genes and the distal locus has 41 genes. My microRNA chip contains 5 of the 10 genes at the proximal locus and 25 of the 41 genes at the distal locus. These 30 genes were significantly down-regulated in GISTs with 14q loss. Therefore, among the 38 down-regulated microRNAs from 14q, 30 were encoded by these two microRNA clusters, and microRNAs from these two loci showed different patterns according to anatomic site. In the five small bowel GISTs with 14q loss, relatively similar or slight down-regulation of the 30 microRNAs was observed compared to the nine stomach GISTs with 14q loss (Fig. 4*b*). To examine the reliability of the array data, we selected six microRNAs (miR-495, miR-376, miR-134, miR-377, miR-539 and miR-154) encoded on 14q and analyzed their expression pattern by RT-PCR (five microRNAs) and Northern blotting (two microRNAs). I found that the expression levels of these microRNAs as analyzed by microarray, RT-PCR, and Northern blotting, were similar (Figs. 4*c* and 4*d*).

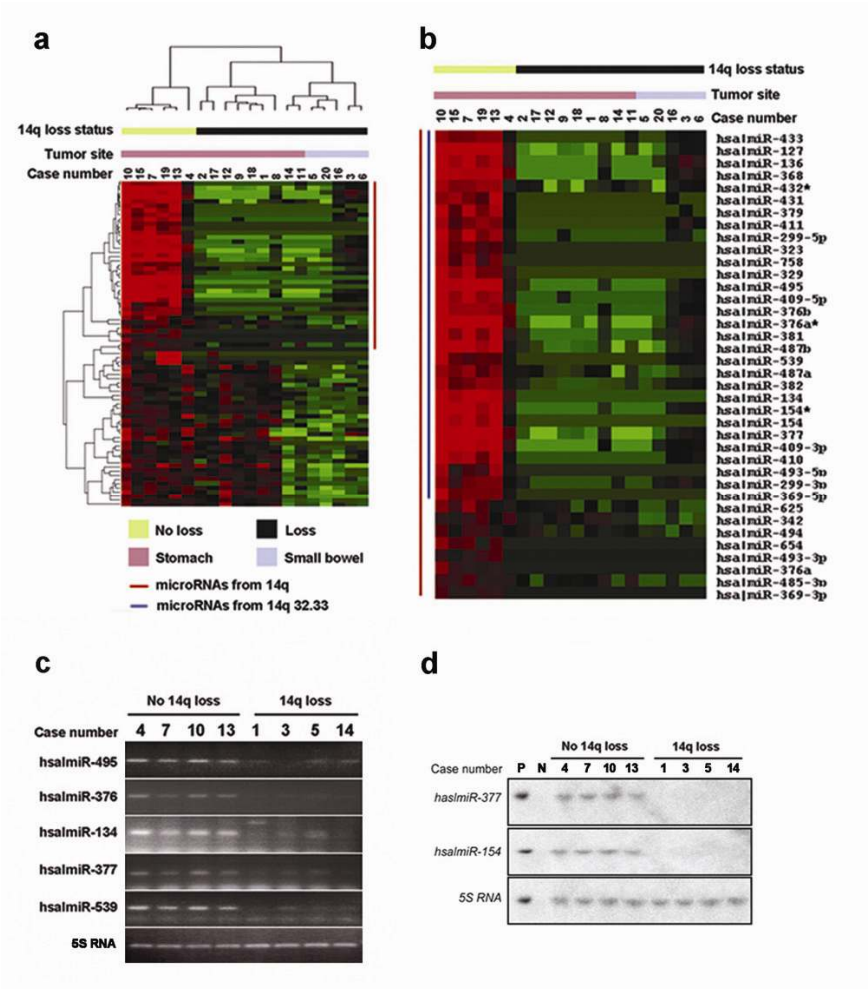

Fig 4. Identification of differentially expressed microRNAs according to the 14q chromosome loss. We ranked the microRNAs using the Mann-Whitney rank sum test. Outlier genes responsible for anatomic site or chromosomal alteration status were selected by $p < 0.05$. In addition, significant outlier subset genes were further narrowed down by filtering genes showing greater than ± 2-fold expression changes. (a) Supervised hierarchical clustering analysis of GISTs using 73 differentially expressed genes. GISTs were separated according to anatomic site and 14q loss status. (b) 30 differentially

expressed microRNAs from two clusters on 14q32.33. Six GISTs lacking 14q loss showed strong microRNA expression while severe down- regulation was noted in nine stomach GISTs with 14q loss. In five small bowel GISTs with 14q loss, mild down-regulation was noted. (c) Validation of microRNA expression by RT-PCR. (d) Validation of microRNA expression by Northern blotting. P and N indicate the positive and negative control, respectively.

5. Relationship between dysregulated microRNAs in GISTs and KIT overexpression

The characteristic molecular changes of GISTs are *KIT* gain-of-function mutations and KIT overexpression.[9,10] Although *KIT* mutations are directly related to KIT activation, the mechanism of KIT overexpression is not well-known. In my 20 cases, the amount of KIT expression was directly related to *KIT* mutations, with the exception of three cases (cases 3, 13, and 15). The association between KIT activation and down-regulation of mir-221 and mir-222 has been reported previously.[30, 31] I hypothesized that microRNAs play an important role in KIT overexpression. First, I used http://www.targetscan.org to search for candidate microRNAs that can bind the 3'UTR region of *KIT* in a site-specific manner and found 111 microRNA candidates. Among these candidates, my microRNA chip contained 62 microRNAs and 16 of these were located on 14q. Expression of these 16 microRNAs was homogeneously down-regulated in 14 GISTs with 14q loss (Fig. 5). I evaluated the relationship between the expression of 62 microRNAs and KIT overexpression. I found that the expression of five microRNAs (mir-510, mir-142-5p, mir-9*, mir-370, and mir-494) was significantly related to KIT

expression (Fig. 5).

I also found that miR-221 and miR-222 were down-regulated; these two microRNAs have previously been reported to be associated with KIT overexpression. In my GISTs, KIT overexpression was found in 14 of 20 cases, and down-regulation of miR-221 and miR-222 was found in 11 of these 14 cases, but this association was not statistically significant.

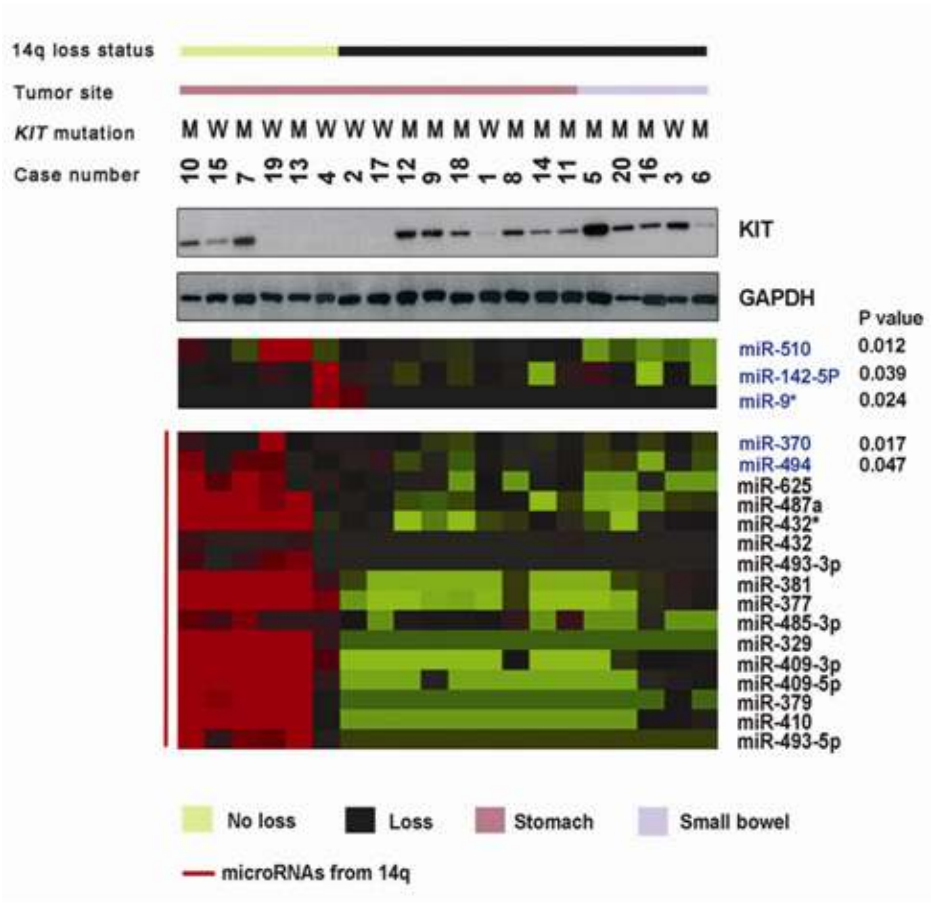

Fig 5. The expression of five microRNAs (two microRNAs from 14q and three microRNAs from other chromosomes) correlated to KIT overexpression in GISTs. Expression of KIT was analyzed by Western blotting and compared to the expression of 62 microRNAs possibly targeting *KIT*. KIT expression was related to *KIT* mutations, and microRNA expression was related to the status of chromosome 14 loss. There was a significant relationship between *KIT* and microRNA expression in 5 of 62 microRNAs ($p < 0.05$, *t*-test). Among the five microRNAs, two microRNAs (miR-370 and miR-494) were located on 14q.

Ⅵ. Discussion

In this study, I analyzed the microRNA expression patterns of 20 GISTs, and investigated the relationship between microRNA expression profiles and genetic changes and clinicopathologic features of GISTs. I found four distinct microRNA expression patterns in our GISTs; these patterns were correlated with 14q chromosomal loss status, anatomic site, and tumor risk. These findings suggest that the microRNA expression patterns of GISTs are related to genomic changes and the biological behavior of the tumor.

GISTs are well-known mesenchymal tumors with unique morphological and genetic characteristics.[32, 33] A previous report described unique genomic alterations and homogeneous mRNA and microRNA expression profiles in GISTs in contrast to other types of sarcomas.[23] These differences might be related to the unique genomic structure of GISTs. Loss of 14q is a unique genomic change in GISTs, and has been reported in more than 70% of GISTs.[16, 20] A strong associations between microRNA expression and genomic changes has been reported in many tumors.[24-26, 34] This unique chromosomal change in GISTs might contribute to the distinct microRNA expression profiles of GISTs compared to other sarcomas.

In this study, I demonstrated that the microRNA expression profile of GISTs is dependent upon the type of chromosomal change, especially 14q loss status and anatomic site. Chromosome 14q contains two large microRNA clusters that have been identified to date. My microRNA expression study demonstrated that the microRNAs encoded by these two clusters on 14q were severely down-regulated in the nine stomach GISTs with 14q loss. I also

found that the down-regulation of microRNAs in 14q was different between stomach and small bowel GISTs. The five small bowel GISTs with 14q loss also showed down-regulation of microRNAs from the two clusters of 14q; however, the intensity of down-regulation was much lower than that observed in the nine stomach GISTs with 14q loss. When I compared the microRNA expression between four stomach and five small bowel GISTs in the high-risk group containing the 14q loss, two microRNAs (mir-136 and mir-409-3p) encoded by 14q were significantly up-regulated and two microRNAs (mir-638 and mir-625) were significantly down-regulated in the small bowel GISTs, although all nine stomach and small bowel GISTs had 14q loss.

GISTs are homogenous mesenchymal tumors of the gastrointestinal tract. However, many pathological and biological differences between stomach and small bowel GISTs have been reported. Histologically, small bowel GISTs occasionally display skeinoid fibers and the organoid feature, which is absent in stomach GISTs. In addition, *PDGFRA*-mutated GISTs, which are known to be of relatively low malignant potential, arise exclusively in the stomach. Small bowel GISTs are high-risk, have higher proliferation rates, and a shorter disease-free survival.[13] The overall tumor-related mortality of small bowel GISTs and their recurrence rate are higher than those of stomach GISTs. Small bowel GISTs, even when of similar size and mitotic count to stomach GISTS, have a worse prognosis.[35] It has been reported that a small bowel location is a predictable factor for recurrence after complete excision of primary GISTs.[36] In addition to these pathological and biological differences, Antonescu *et al*.[37] reported that there was a notable difference in gene expression between stomach and small bowel GISTs. Hierarchical cluster analysis of GISTs

according to location showed two distinct genomic clusters: stomach and small bowel GISTs. This was confirmed using four familial tumors from one patient, two of which were in the stomach and two that were intestinal.[37] Additionally, another study on the gene expression profile of GISTs confirmed that the most determinant factor separating GISTs from the stomach and small bowel in an unsupervised hierarchical clustering was tumor location.[38] The different types of *KIT* mutation that characterizes small bowel and gastric GISTs might contribute to their different gene and microRNA expression patterns. For example, mutation of exon 9 of *KIT* is often found in small bowel GISTs[39]. When I analyzed the microRNA expression profile of our 13 GISTs with *KIT* mutations using unsupervised hierarchical clustering analysis, I found that cases with exon 9 mutations formed a separate cluster. The other cases with exon 11 mutations were subdivided according to 14q loss. Here, I found that small bowel GISTs had unique microRNA expression patterns. Most of the down-regulated microRNAs in small bowel GISTs are known to play a role in the activation of mitogen-activated protein kinase (MAPK) and the cell cycle, suggesting that these microRNA expression differences may be related to the aggressive biologic behavior of small bowel GISTs and may contribute to the differences in biologic behavior between stomach and small bowel GISTs.

My study demonstrated that several microRNAs are differentially expressed according to GIST tumor risk. When I compared 10 high-risk GISTs to 4 low-risk GISTs, I found that 28 microRNAs were significantly down-regulated in the high-risk GISTs. Most of these microRNAs are related to MAPK and the cell cycle, and therefore it is expected that the down-

regulation of these microRNAs will be positively correlated to cell proliferation and tumor progression. Among these microRNAs, miR-125b and miR-21 have been reported to be down-regulated in breast cancer[40] and to be related to tumor stage, proliferation index, and vascular invasion. miR-342 had been reported to be specifically down-regulated in colon cancer according to the adenoma-carcinoma sequence.[41] The down-regulation of miR-342 is due to promoter methylation; in normal mucosa, only 12% of cases were methylated whereas in adenoma, 67% of cases were methylated and the methylation increased to 86% in carcinoma.[41] The methylation of miR-342 results in increased cell proliferation, because silencing of miR-342 inhibits apoptosis. All of these findings indicate that differences in microRNA expression between high-risk and low-risk GISTs can contribute to rapid tumor progression in GISTs in the high-risk group.

Furthermore, I demonstrated that the microRNA expression signatures of my GISTs might be related to KIT overexpression. It is well-known that microRNAs regulate many genes, and tumors can develop with the loss of microRNA regulation. I initially hypothesized that differently expressed microRNAs are important for GIST development. Using *in silico* analysis, I found 111 microRNAs that can bind to *KIT* and myr microRNA chip contained 62 out of these 111 microRNA candidates. These findings raised the possibility that the down-regulation of these microRNAs may be related to KIT overexpression in GISTs. When I compared the expression profiles of the 62 microRNAs with KIT overexpression, I found that KIT overexpression was significantly correlated to the expression of five microRNAs and *KIT* mutations. The role of *KIT* mutations in GIST tumorigenesis is well-known.

KIT is frequently overexpressed and is generally used as a diagnostic marker of GISTs. Although the relationship between *KIT* mutations and KIT overexpression has been demonstrated,[8] some exceptional cases have also been reported.[42] Here, I showed that expression changes in some microRNAs are related to KIT overexpression. These results suggest a possible role of microRNAs in KIT overexpression in GISTs.

In conclusion, I found that microRNA expression patterns can differentiate several subsets of GISTs and are closely related to the presence or absence of 14q, tumor risk, and anatomic site. My findings suggest that microRNA expression profiles can be used for the molecular classifications of GISTs.

Ⅴ. CONCLUSIONS

In order to evaluate the relationship between microRNA expression and clinicopathologic finding of GISTs, I analyzed the microRNA expression profiles of 20 GISTs. I demonstrated that

1. MicroRNA expression patterns of GISTs are associated with anatomic site and tumor risk.

2. The mutation status of *KIT* or *PDGFRA* is not related to the microRNA expression patterns.

3. MicroRNA expression patterm of GISTs is associated with hemizygosity deletion of 14q.

4. The amount of KIT expression is related to *KIT* mutations.

REFERENCES

1. Price VE, Zielenska M, Chilton-MacNeill S, Smith CR, Pappo AS. Clinical and molecular characteristics of pediatric gastrointestinal stromal tumors (GISTs). Pediatr Blood Cancer 2005;45:20-4.

2. Silberman S, Joensuu H. Overview of issues related to imatinib therapy of advanced gastrointestinal stromal tumors: a discussion among the experts. Eur J Cancer 2002;38 Suppl 5:S66-9.

3. Kirsch R, Gao ZH, Riddell R. Gastrointestinal stromal tumors: diagnostic challenges and practical approach to differential diagnosis. Adv Anat Pathol 2007;14:261-85.

4. Cho S, Kitadai Y, Yoshida S, Tanaka S, Yoshihara M, Yoshida K *et al*. Genetic and pathologic characteristics of gastrointestinal stromal tumors in extragastric lesions. Int J Mol Med 2006;18:1067-71.

5. Lasota J, Jasinski M, Sarlomo-Rikala M, Miettinen M. Mutations in exon 11 of c-Kit occur preferentially in malignant versus benign gastrointestinal stromal tumors and do not occur in leiomyomas or leiomyosarcomas. Am J Pathol 1999;154:53-60.

6. Taniguchi M, Nishida T, Hirota S, Isozaki K, Ito T, Nomura T *et al*. Effect of c-kit mutation on prognosis of gastrointestinal stromal tumors. Cancer Res 1999;59:4297-300.

7. Janeway KA, Liegl B, Harlow A, Le C, Perez-Atayde A, Kozakewich H *et al*. Pediatric KIT wild-type and platelet-derived growth factor receptor alpha-wild-type gastrointestinal stromal tumors share KIT activation but not mechanisms of genetic progression with adult gastrointestinal stromal tumors. Cancer Res 2007;67:9084-8.

8. Rubin BP, Singer S, Tsao C, Duensing A, Lux ML, Ruiz R *et al*. KIT activation is a ubiquitous feature of gastrointestinal stromal tumors. Cancer Res 2001;61:8118-21.

9. Nakahara M, Isozaki K, Hirota S, Miyagawa J, Hase-Sawada N, Taniguchi M *et al*. A novel gain-of-function mutation of c-kit gene in gastrointestinal stromal tumors. Gastroenterology 1998;115:1090-5.

10. Hirota S, Isozaki K, Moriyama Y, Hashimoto K, Nishida T, Ishiguro S *et al*. Gain-of-function mutations of c-kit in human gastrointestinal stromal tumors. Science 1998;279:577-80.

11. Heinrich MC, Corless CL, Duensing A, McGreevey L, Chen CJ, Joseph N *et al*. PDGFRA activating mutations in gastrointestinal stromal tumors. Science 2003;299:708-10.

12. Kang HJ, Nam SW, Kim H, Rhee H, Kim NG, Hyung WJ *et al*. Correlation of KIT and platelet-derived growth factor receptor alpha mutations with gene activation and expression profiles in gastrointestinal

stromal tumors. Oncogene 2005;24:1066-74.

13. Gunawan B, von Heydebreck A, Sander B, Schulten HJ, Haller F, Langer C *et al*. An oncogenetic tree model in gastrointestinal stromal tumours (GISTs) identifies different pathways of cytogenetic evolution with prognostic implications. J Pathol 2007;211:463-70.

14. Breiner JA, Meis-Kindblom J, Kindblom LG, McComb E, Liu J, Nelson M *et al*. Loss of 14q and 22q in gastrointestinal stromal tumors (pacemaker cell tumors). Cancer Genet Cytogenet 2000;120:111-6.

15. Assamaki R, Sarlomo-Rikala M, Lopez-Guerrero JA, Lasota J, Andersson LC, Llombart-Bosch A *et al*. Array comparative genomic hybridization analysis of chromosomal imbalances and their target genes in gastrointestinal stromal tumors. Genes Chromosomes Cancer 2007;46:564-76.

16. Wozniak A, Sciot R, Guillou L, Pauwels P, Wasag B, Stul M *et al*. Array CGH analysis in primary gastrointestinal stromal tumors: cytogenetic profile correlates with anatomic site and tumor aggressiveness, irrespective of mutational status. Genes Chromosomes Cancer 2007;46:261-76.

17. Meza-Zepeda LA, Kresse SH, Barragan-Polania AH, Bjerkehagen B, Ohnstad HO, Namlos HM *et al*. Array comparative genomic hybridization

reveals distinct DNA copy number differences between gastrointestinal stromal tumors and leiomyosarcomas. Cancer Res 2006;66:8984-93.

18. El-Rifai W, Sarlomo-Rikala M, Andersson LC, Knuutila S, Miettinen M. DNA sequence copy number changes in gastrointestinal stromal tumors: tumor progression and prognostic significance. Cancer Res 2000;60:3899-903.

19. Sarlomo-Rikala M, El-Rifai W, Lahtinen T, Andersson LC, Miettinen M, Knuutila S. Different patterns of DNA copy number changes in gastrointestinal stromal tumors, leiomyomas, and schwannomas. Hum Pathol 1998;29:476-81.

20. El-Rifai W, Sarlomo-Rikala M, Miettinen M, Knuutila S, Andersson LC. DNA copy number losses in chromosome 14: an early change in gastrointestinal stromal tumors. Cancer Res 1996;56:3230-3.

21. Gunawan B, Bergmann F, Hoer J, Langer C, Schumpelick V, Becker H *et al*. Biological and clinical significance of cytogenetic abnormalities in low-risk and high-risk gastrointestinal stromal tumors. Hum Pathol 2002;33:316-21.

22. Kang HJ, Koh KH, Yang E, You KT, Kim HJ, Paik YK *et al*. Differentially expressed proteins in gastrointestinal stromal tumors with KIT and PDGFRA mutations. Proteomics 2006;6:1151-7.

23. Subramanian S, Lui WO, Lee CH, Espinosa I, Nielsen TO, Heinrich MC *et al*. MicroRNA expression signature of human sarcomas. Oncogene 2008;27:2015-26.

24. Connolly E, Melegari M, Landgraf P, Tchaikovskaya T, Tennant BC, Slagle BL *et al*. Elevated expression of the miR-17-92 polycistron and miR-21 in hepadnavirus-associated hepatocellular carcinoma contributes to the malignant phenotype. Am J Pathol 2008;173:856-64.

25. Kumar MS, Lu J, Mercer KL, Golub TR, Jacks T. Impaired microRNA processing enhances cellular transformation and tumorigenesis. Nat Genet 2007;39:673-7.

26. Ladeiro Y, Couchy G, Balabaud C, Bioulac-Sage P, Pelletier L, Rebouissou S *et al*. MicroRNA profiling in hepatocellular tumors is associated with clinical features and oncogene/tumor suppressor gene mutations. Hepatology 2008;47:1955-63.

27. Kim NG, Kim JJ, Ahn JY, Seong CM, Noh SH, Kim CB *et al*. Putative chromosomal deletions on 9P, 9Q and 22Q occur preferentially in malignant gastrointestinal stromal tumors. Int J Cancer 2000;85:633-8.

28. Fletcher CD, Berman JJ, Corless C, Gorstein F, Lasota J, Longley BJ *et al*. Diagnosis of gastrointestinal stromal tumors: A consensus approach. Hum Pathol 2002;33:459-65.

29. Lux ML, Rubin BP, Biase TL, Chen CJ, Maclure T, Demetri G *et al*. KIT extracellular and kinase domain mutations in gastrointestinal stromal tumors. Am J Pathol 2000;156:791-5.

30. Felicetti F, Errico MC, Bottero L, Segnalini P, Stoppacciaro A, Biffoni M *et al*. The promyelocytic leukemia zinc finger-microRNA-221/-222 pathway controls melanoma progression through multiple oncogenic mechanisms. Cancer Res 2008;68:2745-54.

31. Felli N, Fontana L, Pelosi E, Botta R, Bonci D, Facchiano F *et al*. MicroRNAs 221 and 222 inhibit normal erythropoiesis and erythroleukemic cell growth via kit receptor down-modulation. Proc Natl Acad Sci U S A 2005;102:18081-6.

32. Yang J, Du X, Lazar AJ, Pollock R, Hunt K, Chen K *et al*. Genetic aberrations of gastrointestinal stromal tumors. Cancer 2008;113:1532-43.

33. Hirota S, Isozaki K. Pathology of gastrointestinal stromal tumors. Pathol Int 2006;56:1-9.

34. Huppi K, Volfovsky N, Mackiewicz M, Runfola T, Jones TL, Martin SE *et al*. MicroRNAs and genomic instability. Semin Cancer Biol 2007;17:65-73.

35. Miettinen M, Makhlouf H, Sobin LH, Lasota J. Gastrointestinal stromal tumors of the jejunum and ileum: a clinicopathologic,

immunohistochemical, and molecular genetic study of 906 cases before imatinib with long-term follow-up. Am J Surg Pathol 2006;30:477-89.

36. Dematteo RP, Gold JS, Saran L, Gonen M, Liau KH, Maki RG *et al*. Tumor mitotic rate, size, and location independently predict recurrence after resection of primary gastrointestinal stromal tumor (GIST). Cancer 2008;112:608-15.

37. Antonescu CR, Viale A, Sarran L, Tschernyavsky SJ, Gonen M, Segal NH *et al*. Gene expression in gastrointestinal stromal tumors is distinguished by KIT genotype and anatomic site. Clin Cancer Res 2004;10:3282-90.

38. Yamaguchi U, Nakayama R, Honda K, Ichikawa H, Hasegawa T, Shitashige M *et al*. Distinct gene expression-defined classes of gastrointestinal stromal tumor. J Clin Oncol 2008;26:4100-8.

39. Lasota J, Wozniak A, Sarlomo-Rikala M, Rys J, Kordek R, Nassar A *et al*. Mutations in exons 9 and 13 of KIT gene are rare events in gastrointestinal stromal tumors. A study of 200 cases. Am J Pathol 2000;157:1091-5.

40. Iorio MV, Ferracin M, Liu CG, Veronese A, Spizzo R, Sabbioni S *et al*. MicroRNA gene expression deregulation in human breast cancer. Cancer Res 2005;65:7065-70.

41. Grady WM, Parkin RK, Mitchell PS, Lee JH, Kim YH, Tsuchiya KD *et al*. Epigenetic silencing of the intronic microRNA hsa-miR-342 and its host gene EVL in colorectal cancer. Oncogene 2008;27:3880-8.

42. Medeiros F, Corless CL, Duensing A, Hornick JL, Oliveira AM, Heinrich MC *et al*. KIT-negative gastrointestinal stromal tumors: proof of concept and therapeutic implications. Am J Surg Pathol 2004;28:889-94.

< ABSTRACT (IN KOREAN)>

위장관간질종양에서 보이는 microRNA 발현 양상 차이비교

<지도교수 김호근>

연세대학교 대학원 의과학과

최 희 정

microRNA는 유전자 발현을 조절하는 것으로 알려져 있다. 이러한 microRNA의 독특한 발현 양상은 여러 유형의 종양에서 관찰되었지만 위장관간질종양에서 보여지는 발현 양상에 대해서는 거의 보고되지 않았다. 위장관간질종양은 대표적인 간엽성 종양(mesenchymal tumor)으로 약 80%의 위장관간질종양에서 v-kit Hardy-Zuckerman 4 feline sarcoma viral oncogene homolog (KIT) 종양형성유전자의 gain-of-function 돌연변이가 있음이 관찰되었다. 또한 *KIT* 유전자 돌연변이가 없는 위장관간질종양 중 약 35%에서 platelet-derived growth factor receptor α (PDGFRA) 유전자 돌연변이가 있음이 확인되었다. 따라서 이 두 유전자의 돌연변이 유무에 따른 microRNA 발현 양상을 비교함으로써 위장관간질종양에서 나타나는 임상병리학적인 특징을

찾을 수 있을 것으로 예상된다. 또한 약 70%의 위장관간질종양에서 보여지는 14번 염색체 손실과 그로 인한 종양 위험군에 따라 종양세포의 형태나 크기, 분열능 등의 분자적, 임상병리학적 특징과 위장관간질종양에서 빈번하게 보여지는 *KIT* 유전자의 돌연변이 유무와 과발현 사이에서 보여지는 microRNA 발현 양상을 비교하여 실제 조절 가능한 유전자에 관한 규명이 필요하게 되었다.

본 연구에서는 위장관간질종양에서 *KIT* 및 *PDGFRA* 유전자의 변이 및 여러 임상유전학적 특성에 따른 microRNA 발현 양상의 변화를 검증하기 위하여 전체 20예의 위장관간질종양 환자의 조직을 대상으로 miroRNA microarray 검사를 수행하였다. 20예의 위장관간질종양 환자의 조직은 뚜렷하게 4개의 그룹으로 구분되었고, 이 중 6예는 14번 염색체 손실이 없었으며, 나머지 14예의 위장관간질종양은 14번 염색체의 손실을 보였다. 염색체 손실을 보인 14예의 위장관간질종양은 또한 염색체 손실과 종양 위험군 (tumor-risk) 에 따라 2개의 그룹으로 나눠졌다. 그리고 14번 염색체 손실이 있는 위장관간질종양에서 73개의 microRNA 가 의미 있게 감소하였으며, 이 중 38개의 microRNA 가 14번 염색체에 존재하는 것임을 확인하였다. 또한 많은 microRNA가 종양 기원 및 위험군에 따라 다른 발현 양상을 보이며 특히 소장 (small bowel) 기원의 고위험군 (high-risk)에서 발현량이 현저히 감소하는 것을 확인하였다.

이와 함께 위장관간질종양에서 돌연변이를 변이를 보이는 *KIT* 유전자 조절에 관련된 microRNA 요인을 확인하기 위해 in silico 분석을 통해 *KIT* 유전자 조절에 관여할 것으로 여겨지는 111개의 candidate microRNA 를 여과하였다. 이 중 통계적 분석에 따라 *KIT* 유전자 조절에 관여하는 5개의 microRNA (miR-510, miR-142-5p, miR-9*, miR-370 과 miR-494) 를 확인하였다.

결론적으로 본 연구는 위장관간질종양에서 보이는 염색체 손실과 그로 인한 microRNA 발현 패턴을 분석함으로써 분자생물학적 특징과 임상병리학적 특징에 관한 연관성을 규명하였다. 또한 실제 위장관간질종양에서 돌연변이를 보이는 *KIT* 유전자의 조절에 관여하는 microRNA를 확인했다. 이러한 연구결과는 위장관간질종양에서 microRNA 발현과 이와 밀접하게 연관된 임상병리학적 특징을 통해 위장관간질종양의 분자생물학적 특징과 분류에 기여할 것으로 여겨지며, 또한 *KIT* 유전자의 작용 기작 및 조절에 관여하는 microRNA를 밝혀냄으로써, 위장관간질종양 뿐만 아니라 다른 암에서의 임상적, 병리학적, 분자생물학적 특징에 따른 특화된 암 치료법 개발에 기여하리라 사료된다.

핵심되는 말: microRNA, 위장관 간질 종양, *KIT*, 14 번 유전자 손실, 발현 프로파일링

PUBLICATION LISTS

1. Kang HJ, Lee H, Choi HJ, Youn JH, Shin JS, Ahn YH *et al*. Non-histone nuclear factor HMGB1 is phosphorylated and secreted in colon cancers. Lab Invest. 2009;89(8):948-59

2. Choi HJ, Lee H, Kim H, Kwon JE, Kang HJ, You KT *et al*. MicroRNA expression profile of gastrointestinal stromal tumors is distinguished by 14q loss and anatomic site. Int J Cancer. 2009 (Epub ahead of print)